Testing the gauged $U(1)_{B-L}$ model for loop induced neutrino mass with dark matter at future colliders

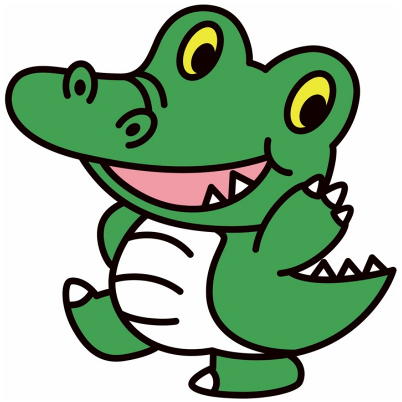

大阪大学
OSAKA UNIVERSITY

Guohao Ying

paper in preparation

Department of Physics, Graduate School of Science, Osaka University

Collaborator: Prof. ***Shinya Kanemura*** (Osaka U.), ***Yushi Mura*** (Osaka U.)

LCWS2024@UTokyo, July 9th, 2024

1. Introduction: What we have already known?

The Standard Model

- Discovery of the Higgs boson in the LHC

- All particles in the SM have been verified by experiments

BSM phenomena

- **The origin and smallness of neutrino mass**
- **The nature of dark matter**
- The matter-antimatter asymmetry in the universe

2. Seesaw models

❑ Type-I seesaw

[Minkowski,1977, Yanagida,1979, M Gell-Mann,1979]

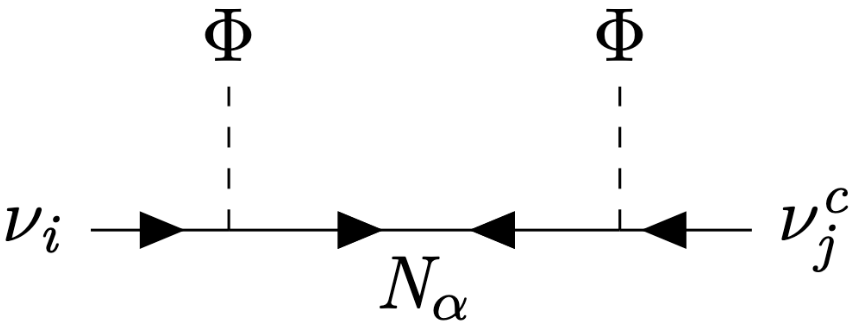

Figure 1: Neutrino mass in Type-I seesaw

$$m_\nu = m_D M^{-1} m_D^T \approx \frac{m_D^2}{M} \approx \frac{y^2 v^2}{2M}$$

In order to realize 0.01 eV neutrino mass:

1. $y \sim 0.1, M \sim 10^{13}$ GeV, difficult to be tested
2. $y \sim 10^{-11}, M \sim 1$ TeV, serious hierarchy problem

❑ Radiative seesaw (Tao-Ma model)

[Z. Tao, 1996, E. Ma, 2006] (Explain neutrino mass and DM simultaneously)

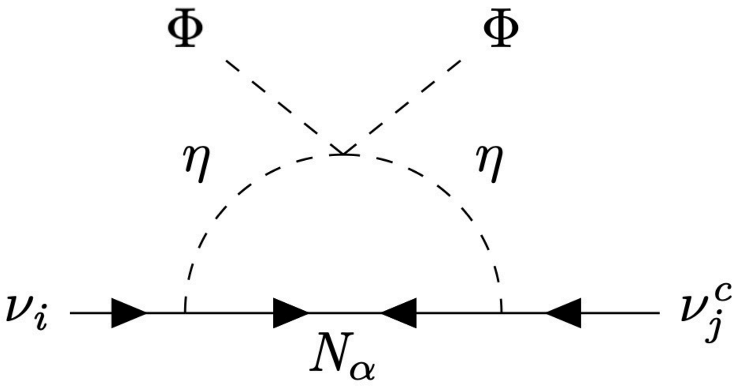

Figure 2: One-loop generation of neutrino mass in Ma model

$$m_\nu = \frac{\lambda_5 v^2}{32\pi^2} \frac{y y^T}{M} f_{\rm loop}$$

$y \sim 10^{-2}, \lambda_5 \sim 10^{-5}, M \sim 1\,TeV$ ⇨ $m_\nu \sim$ 0.01 eV

1. Unknown mass origin of RH neutrinos.
2. Insufficient annihilation rate for N_1 DM due to strong experimental constraints of charged lepton flavor violation[J. Kubo, E. Ma, D. Suematsu,2006]. (Scalar DM only)

3. Radiative seesaw with a $U(1)_{B-L}$ gauge symmetry

[Kanemura, Seto, Shimomura, 2011]

- New symmetries: an unbroken Z_2 symmetry and a $U(1)_{B-L}$ gauge symmetry
- New fields: 3 Z_2-odd RH neutrinos, a Z_2-odd scalar doublet field η and a Z_2-even scalar singlet field S

	$\mathrm{SU(3)_C}$	$\mathrm{SU(2)_L}$	$\mathrm{U(1)_Y}$	$\mathrm{U(1)_{B-L}}$	$\mathbb{Z}_2$
N_α	$\mathbf{1}$	$\mathbf{1}$	0	-1	$-$
η	$\mathbf{1}$	$\mathbf{2}$	1	0	$-$
S	$\mathbf{1}$	$\mathbf{1}$	0	2	$+$

Table 1: Particle table of this model

$$\mathcal{L}_N = \sum_{\alpha=1}^{3}\left(\sum_{i=1}^{3} g_{i\alpha}\overline{L}_i\tilde{\eta}N_\alpha + \overline{N}_\alpha(i\not{D})N_\alpha - \frac{y_\alpha^R}{2}\overline{N}_\alpha S N_\alpha^c + \text{h.c.}\right)$$

$$\mathcal{L}_{\text{scalar}} = (D_\mu\eta)^\dagger D^\mu\eta + (D_\mu S)^\dagger D^\mu S \quad D_\mu = \partial_\mu - \frac{ig}{2}\tau^a W_\mu^a - \frac{ig'}{2}YB_\mu - ig_{B-L}(B-L)Z'_\mu.$$

$$V(\Phi,\eta,S) = \mu_1^2|\Phi|^2 + \mu_2^2|\eta|^2 + \mu_S^2|S|^2 + \lambda_1|\Phi|^4 + \lambda_2|\eta|^4 + \lambda_S|S|^4 + \lambda_3|\Phi|^2|\eta|^2 + \lambda_4\left|\Phi^\dagger\eta\right|^2 + \frac{\lambda_5}{2}\left[(\Phi^\dagger\eta)^2 + \text{h.c.}\right] + \tilde{\lambda}|\Phi|^2|S|^2 + \lambda|\eta|^2|S|^2$$

$\mu_1^2, \mu_S^2 < 0, \mu_2^2 > 0$

⇓

v, v_S, μ_2^2

This model can explain neutrino mass and dark matter simultaneously

Discovery of Higgs ⇒

- New benchmark scenarios are available.
- It can be tested by future experiments.

4. Neutrino masses

❑ Masses of RH neutrinos

SSB of the $U(1)_{B-L}$ gauge symmetry

$$m_{N_\alpha} = \frac{y_\alpha^R}{\sqrt{2}} v_S$$

B-L gauge boson Z': $m_{Z'} = 2g_{B-L}v_S$

- LEP bounds: $v_S > 3{\sim}3.5$ TeV [Carena, et al, 2004]
- LHC search: Strong constraints for $m_{Z'} < 5.1$ TeV [G. Aad, et al. 2019]

❑ Masses of LH neutrinos

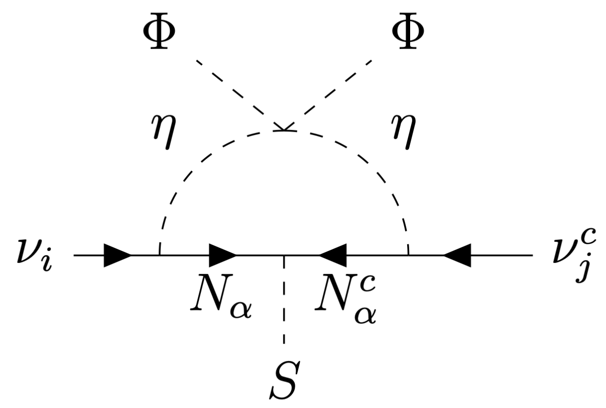

Figure 3: One-loop generation of neutrino mass in $U(1)_{B-L}$ model

$$m_\nu^{ij} = \frac{\lambda_5 v_S}{32\sqrt{2}\pi^2}\left(\frac{v}{m_0}\right)^2 \sum_\alpha g_{j\alpha} g_{i\alpha} y_\alpha^R \quad m_0^2 = \frac{m_H^2 + m_A^2}{2}$$

$y^R \sim 10^{-3}, \frac{v}{m_0} \sim 1, \lambda_5 \sim 10^{-6}, g \sim 10^{-2}, m_\nu^{ij} \sim 10^{-2}$ eV

- SSB of $U(1)_{B-L}$ gauge symmetry ⇒ Mass of RH neutrinos
- EWSB and SSB of $U(1)_{B-L}$ gauge symmetry ⇒ Mass of LH neutrinos

5. Charged lepton flavor violation (CLFV)

- CLFV is strongly suppressed by the square of neutrino masses in the SM [Ardu, Pezzullo, 2022], but it can be enhanced by $N - \eta$ loops in the $U(1)_{B-L}$ model [Toma, Vicente, 2014].

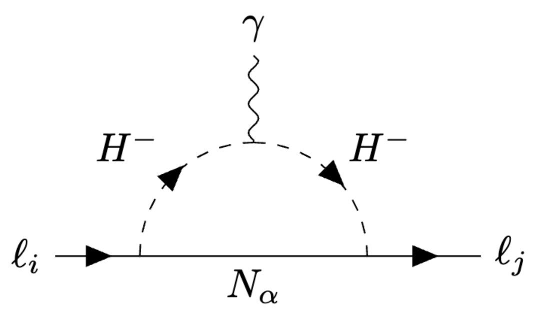

(a)

- Benchmark point:

$\Delta m^2_{21} = (7.53 \pm 0.18) \times 10^{-5}\ eV^2$

$\Delta m^2_{32} = (2.45 \pm 0.03) \times 10^{-3}\ eV^2$

[PDG, 2024]

$m_{H^\pm} = 400$ GeV $\lambda_4 = 0.01$ $\lambda_5 = 10^{-6}$

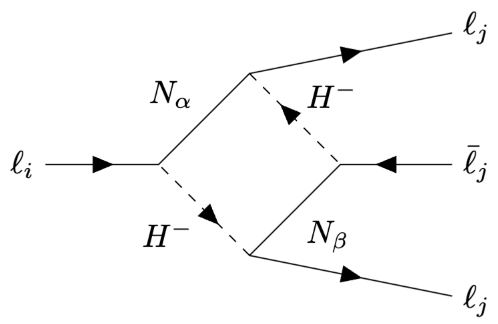

(b)

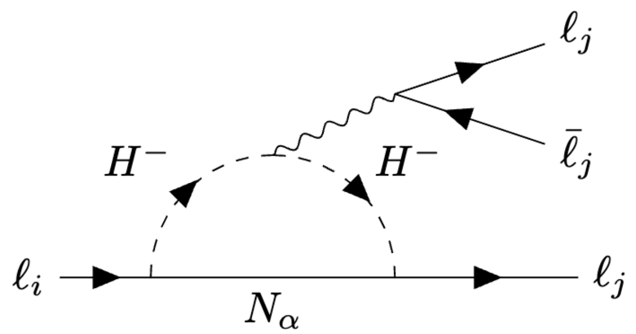

(c)

Figure 4: CLFV process in the $U(1)_{B-L}$ model. (a) radiative diagram. (b) box diagram. (c) penguin diagram.

➢ Numerical results for degenerate RH neutrino masses:

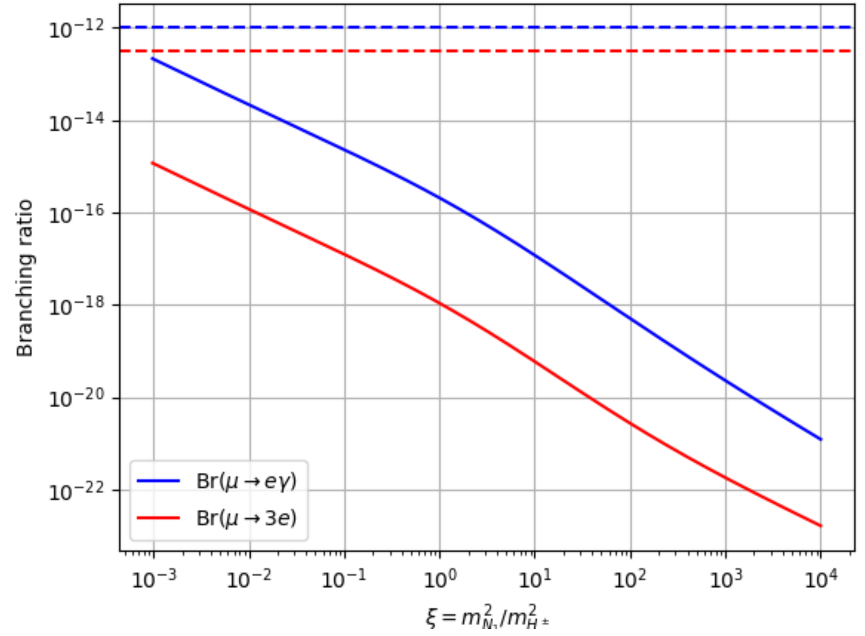

Figure 5: Braching ratios of $\mu \to e\gamma$ and $\mu \to 3e$. The dashed lines are current experiment bounds[MEG II, 2023], [SINDRUM, 1987].

5. Charged lepton flavor violation (CLFV)

➢ Numerical results for non-degenerate RH neutrinos:

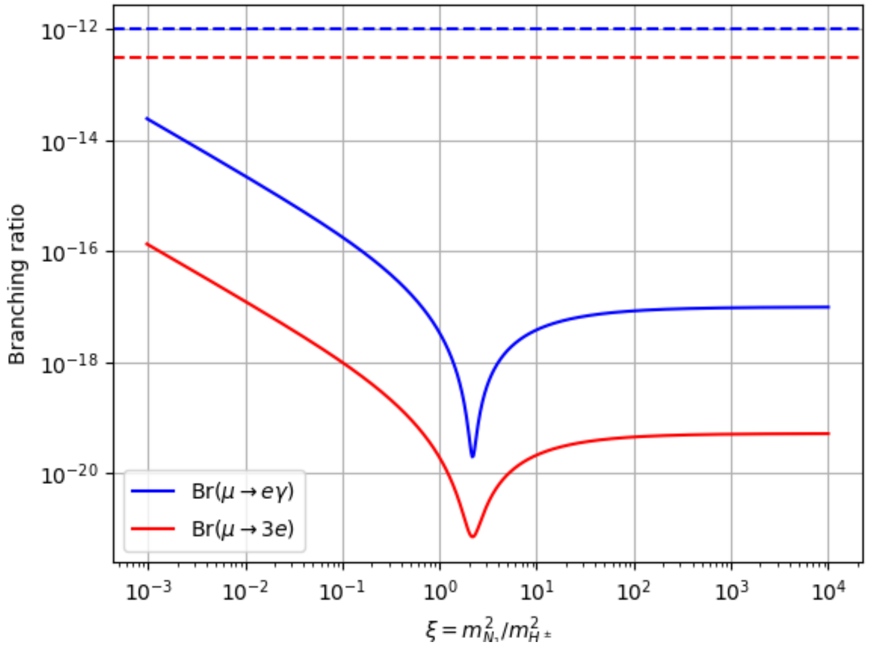

Figure 6: Braching ratios of $\mu \to e\gamma$ and $\mu \to 3e$. The dashed lines are current experiment bounds[MEG II, 2023], [SINDRUM, 1987].

- λ_5: Magnitude of CLFV branching ratios
- m_{N_2}, m_{N_3}: Produce the strong suppression
- $m_{H^\pm}$: Location of the suppression point

❑ Benchmark point:

$\Delta m_{21}^2 = (7.53 \pm 0.18)\times 10^{-5}\ eV^2$

$\Delta m_{32}^2 = (2.45 \pm 0.03)\times 10^{-3}\ eV^2$ [PDG, 2024]

$m_{H^\pm} = 400$ GeV $m_{N_2} = 1000$ GeV $m_{N_3} = 3000$ GeV

$\lambda_4 = 0.01 \quad \lambda_5 = 10^{-6}$

❑ Maximal suppression condition:

$$\frac{m_\nu^2 F(\xi_2)}{\Lambda_2} = \frac{m_\nu^3 F(\xi_3)}{\Lambda_3}$$

$$\Lambda_\alpha = \frac{m_{N_\alpha}}{32\pi^2}\left[\frac{r_h}{\xi_\alpha - r_h}\ln\left(\frac{\xi_\alpha}{r_h}\right) - \frac{r_a}{\xi_\alpha - r_a}\ln\left(\frac{\xi_\alpha}{r_a}\right)\right],$$

$$r_h = 1 + \frac{(\lambda_4 + \lambda_5)v^2}{2m_{H^\pm}^2} \quad r_a = 1 + \frac{(\lambda_4 - \lambda_5)v^2}{2m_{H^\pm}^2} \quad \xi_\alpha = \frac{m_{N_\alpha}^2}{m_{H^\pm}^2}.$$

6. Dark matter (Relic density)

❖ Enough co-annihilation rate for N_1

Mixing between ϕ and ϕ_S:

$$\begin{pmatrix} h_1 \\ h_2 \end{pmatrix} = \begin{pmatrix} \cos\alpha & -\sin\alpha \\ \sin\alpha & \cos\alpha \end{pmatrix} \begin{pmatrix} \phi \\ \phi_S \end{pmatrix}.$$

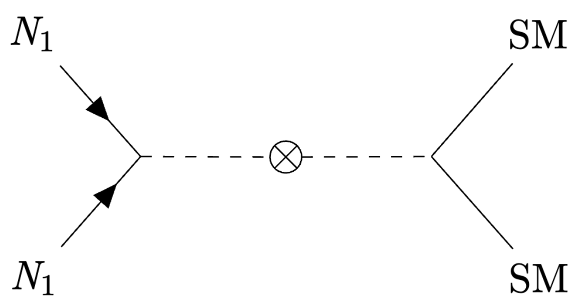

❑ Benchmark point:

$m_{h_1} = 125.25$ GeV

$m_{h_2} = 200$ GeV

$\cos\alpha = 0.95$

Extra s-channel contribution in this model

➢ Numerical results:

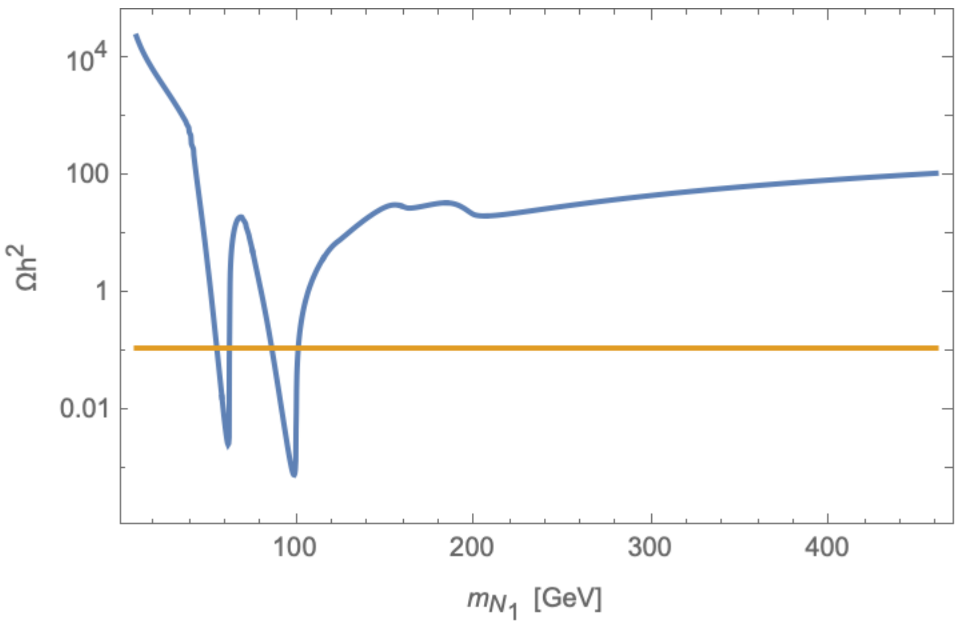

Figure 7: Thermal relic density as a function of m_{N_1}. The yellow line is current bound from Planck experiment [Planck, 2018].

7. Parameter space of this model

For direct search, the spin independent cross section in this model is

$$\sigma_{SI} \propto [\sin(2\alpha)\,(m_{N_1}/v_S)]^2$$

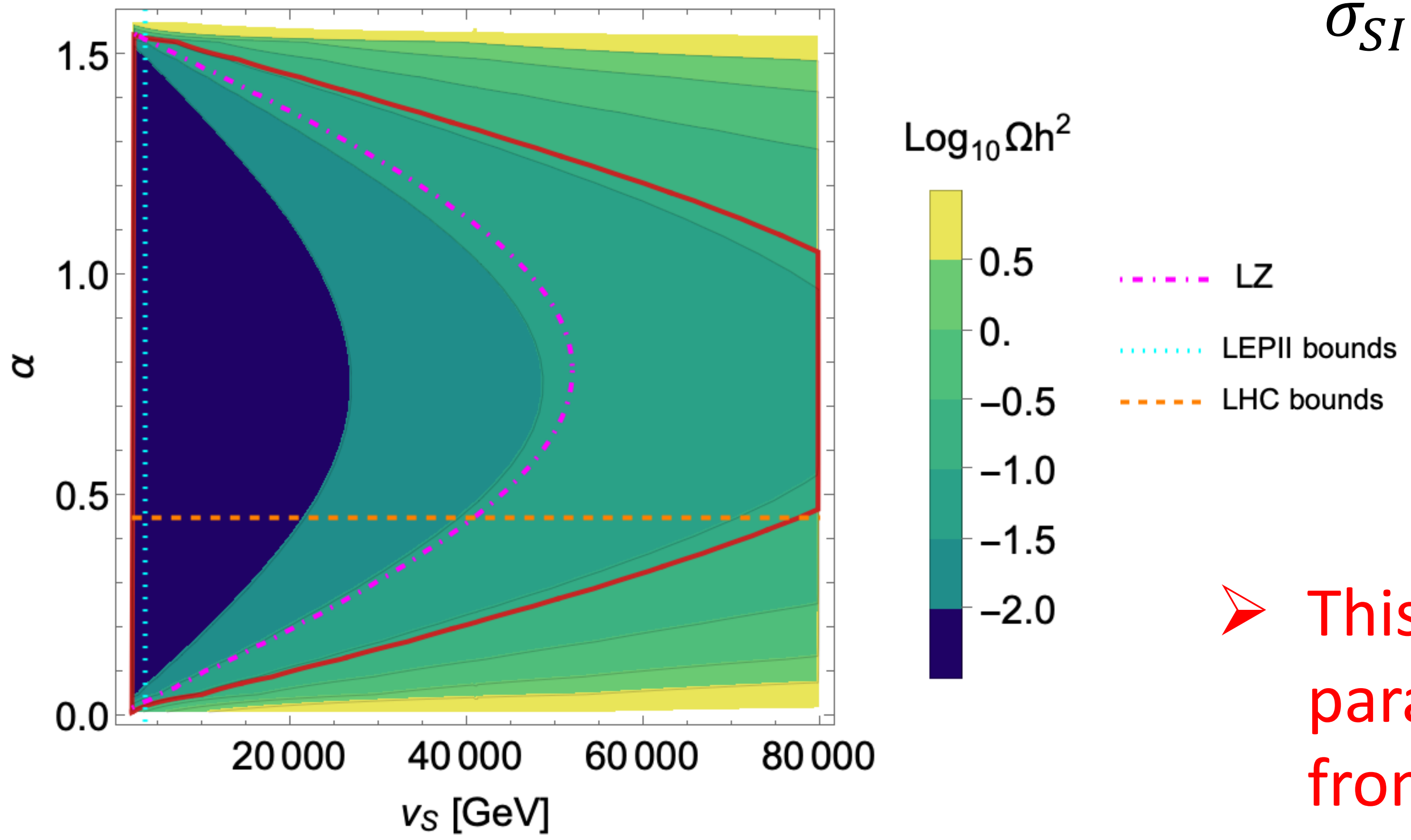

- Benchmark point:

m_{N_1} = 100.2 GeV

m_{N_2} = 2 TeV

m_{N_3} = 5 TeV

m_{h_2} = 200 GeV

➢ This model still has allowed parameter space with constraints from latest experiments.

Figure 8: Current parameter space for U(1)B-L model with constraints from LEPII [Carena, et al, 2004], ATLAS[Aad, et al, 2022] and CMS [Tumasyan, et al, 2022]. The red line is the bound of the relic density of the universe [Planck, 2018]. The dashed pink line is the current bound from the LZ experiment [LZ,2023].

8. DM searches in hadron colliders

- Inert scalar DM: pp $\rightarrow Z^{0*}j \rightarrow HAj$, pp $\rightarrow h_1 j \rightarrow HHj$

Benchmark points				LHC cross sections [$\sqrt{s} = 13$ TeV]	
m_H [GeV]	m_A [GeV]	λ_L	λ_2	$\sigma_{pp\rightarrow HAj}$ [fb]	$\sigma_{pp\rightarrow HHj}$ [fb]
55.	63.	10^{-4}	1.0	92.4	0.0167
55.	63.	0.027	1.0	92.4	878
50.	150.	0.015	1.0	17.8	411

[A. Belyaev, et al, 2018]

$\lambda_L = \lambda_3 + \lambda_4 + \lambda_5$

- RH neutrino DM: pp $\rightarrow H^+H^- \rightarrow N_1 N_1 \overline{l_i} l_j$

Inert charged scalar masses	LHC cross sections [$\sqrt{s} = 13$ TeV]
$m_{H^\pm}$ [GeV]	$\sigma_{pp\rightarrow H^+H^-}$ [fb]
255.3	11.01
395.8	2.50

[A. Ghosh, et al, 2022]

9. DM searches in lepton colliders

[S. Kanemura, et al, 2013]

- Inert scalar DM: $e^+e^- \to Z^{0*} \to HA, e^+e^- \to Z^{0*} \to H^+H^-$

Inert scalar masses			ILC cross sections [$\sqrt{s}$ = 250 GeV (500 GeV)]	
m_H [GeV]	m_A [GeV]	$m_{H^\pm}$ [GeV]	$\sigma_{e^+e^-\to HA}$ [fb]	$\sigma_{e^+e^-\to H^+H^-}$ [fb]
65.	73.	120.	152.(47.)	11. (79.)
65.	120.	120.	74.(41.)	11.(79)

- RH neutrino DM: $e^+e^- \to Z^{0*} \to H^+H^-$

Inert charged scalar masses	ILC cross sections [$\sqrt{s}$ = 250 GeV (500 GeV)]
$m_{H^\pm}$ [GeV]	$\sigma_{e^+e^-\to H^+H^-}$ [fb]
120.	11. (79.)
160.	0. (53)

9. Higgs physics in hadron and lepton colliders

➢ h_1 invisible decay

$$\mathrm{Br}(h_1 \to \text{ invisible}) = \frac{\Gamma_{h_1 \to N_1 N_1}}{\Gamma_{h_1 \to N_1 N_1} + \Gamma_{h_1 \to \mathrm{SM\ particles}}}$$

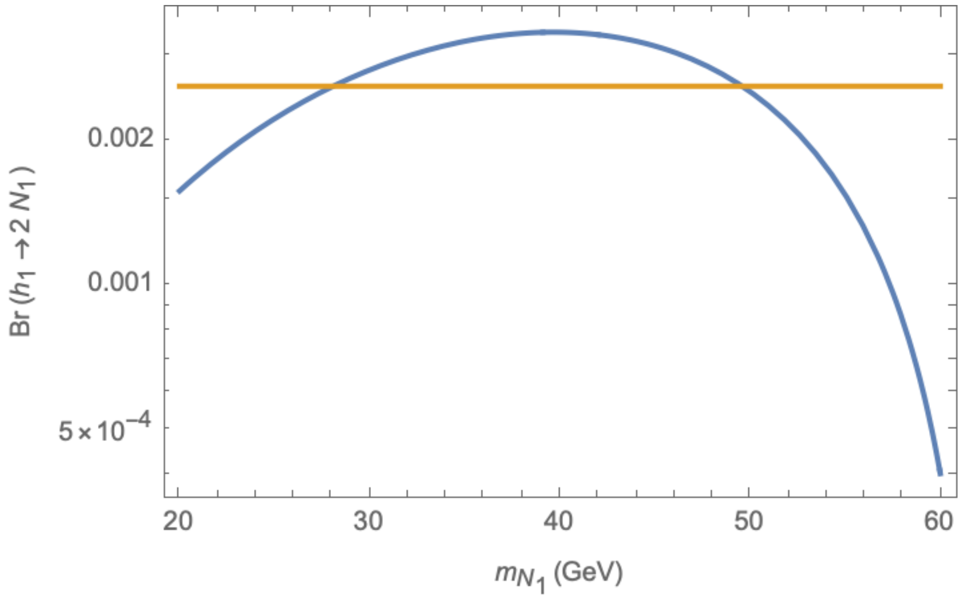

Figure 9: Invisible decay of SM-like Higgs as a function of m_{N_1}. We choose $v_S = 8$ TeV and $cos\alpha = 0.9$ here. The current measured invisible decay branching ratio upper bound is 10.7%[arxiv:2301.10731]. The yellow line is the upper bound in ILC, which is 0.26%[A. Ishikawa, 2019].

➢ h_2 productions

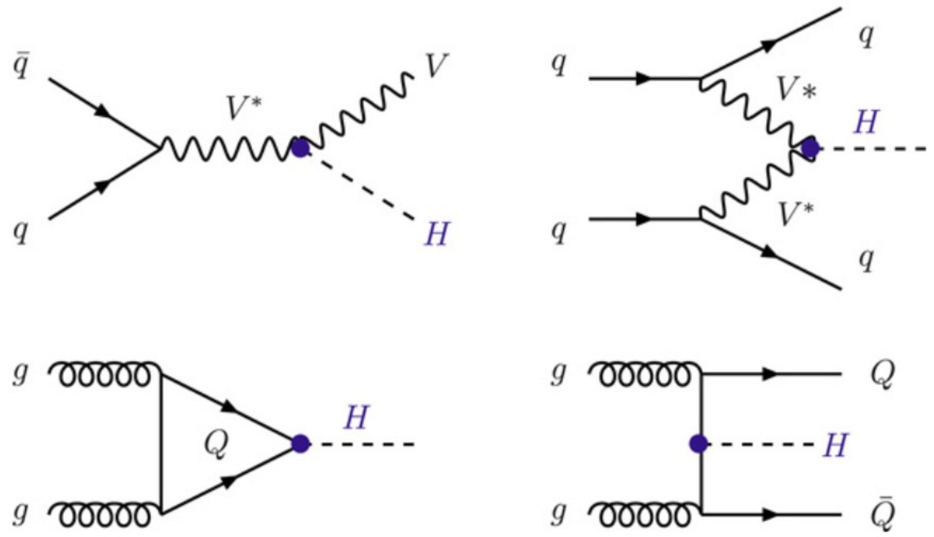

Figure 10: Higgs boson production process in hadron colliders. H can be SM-like Higgs h_1 or the B-L Higgs h_2.

➢ SM-like Higgs boson and B-L Higgs boson are produced through the same processes, the main difference are their masses and the mixing angle factors.

10. Z' boson searches in hadron and lepton colliders

- Z' boson searches in the LHC

$$pp \to Z'X \to \bar{l}lX$$

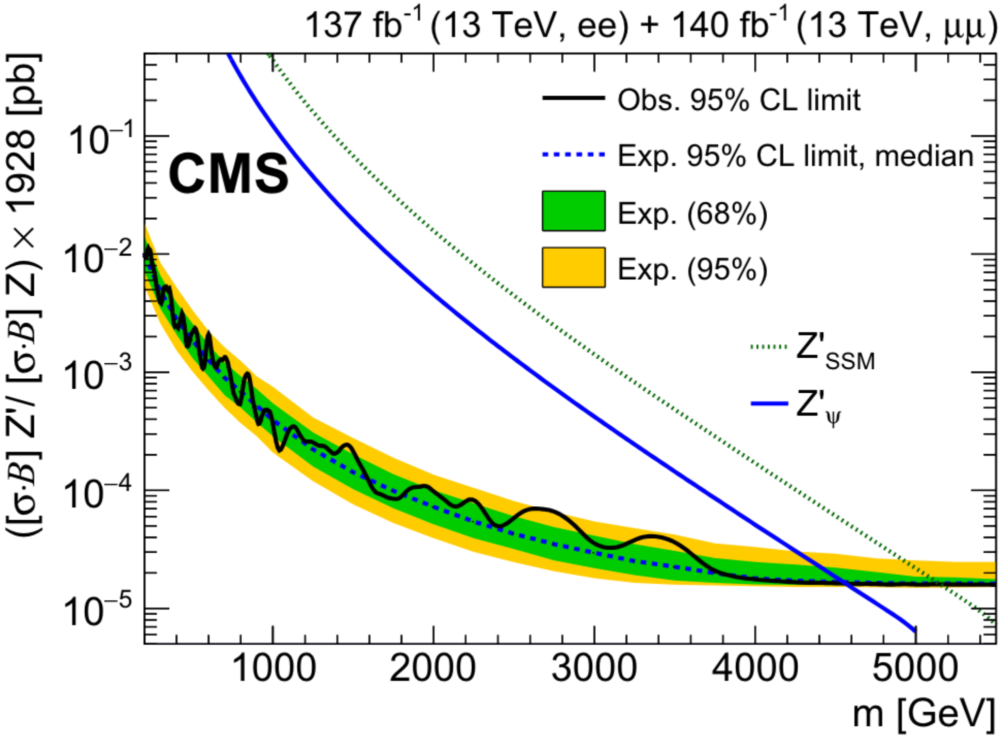

Figure 11:The upper limits at 95% CL on the product of the production cross section and the branching fraction for a spin-1 resonance with a width equal to 0.6% of the resonance mass[arxiv: 2103.02708], where g_q =0.1, $g_l = 0.01$.

- Z' boson searches in the LC

$$e^+e^- \to Z' \to \bar{l}l$$

$M_{Z'}$ (TeV)	g_{B-L}		
	LHC	LC ($\sqrt{s} = 3$ TeV)	LC ($\sqrt{s} = M_{Z'} + 10$ GeV)
1.0	7.1×10^{-3}	5.0×10^{-3}	2.6×10^{-3}
1.5	1.1×10^{-2}	4.0×10^{-3}	3.2×10^{-3}
2.0	1.8×10^{-2}	2.8×10^{-3}	3.4×10^{-3}
2.5	2.8×10^{-2}	2.2×10^{-3}	3.5×10^{-3}

Table: Minimum g_{B-L} value accessible at the LHC and a LC in the B-L model, Luminosity $L = 100\ fb^{-1}$ for LHC and $L = 500\ fb^{-1}$ for LC. [A. Belyaev, 2009].

- LC can reach smaller gauge coupling constants.

10. Results

- We investigated parameter spaces for the radiative seesaw model with a $U(1)_{B-L}$ gauge symmetry with the latest available experimental data and found this model is still feasible from these constraints.
- This model is highly testable in future experiments, including hadron and lepton colliders, DM searches and flavor experiments.

11. Future work

- We will search possible baryogenesis scenarios for this model and give benchmark studies of these scenarios.

Thank you for listening!

Back up

1. Mass spectrum of particles

The $\mathbb{Z}_2$-odd scalar doublet field η can be parameterized as

$$\eta = \begin{pmatrix} H^+ \\ \frac{1}{\sqrt{2}}(H + iA) \end{pmatrix}.$$

The mass spectrum of new particles is

$$\begin{aligned} m_{N_\alpha} &= \frac{y_\alpha^R v_S}{\sqrt{2}}, \\ m_{Z'} &= 2 g_{B-L} v_S, \\ m_{H^\pm}^2 &= \mu_2^2 + \frac{\lambda}{2} v_S^2 + \frac{\lambda_3}{2} v^2, \\ m_H^2 &= \mu_2^2 + \frac{\lambda}{2} v_S^2 + \frac{\lambda_3 + \lambda_4 + \lambda_5}{2} v^2, \\ m_A^2 &= \mu_2^2 + \frac{\lambda}{2} v_S^2 + \frac{\lambda_3 + \lambda_4 - \lambda_5}{2} v^2. \end{aligned}$$

The Higgs field ϕ can mix with the scalar singlet field ϕ_S.

$$\begin{aligned} V(\Phi, S) &\supset \lambda_1 v^2 \phi^2 + \lambda_S v_S^2 \phi_S^2 + \widetilde{\lambda} v v_S \phi \phi_S \\ &= \frac{1}{2} \begin{pmatrix} \phi & \phi_S \end{pmatrix} \begin{pmatrix} 2\lambda_1 v^2 & \widetilde{\lambda} v v_S \\ \widetilde{\lambda} v v_S & 2\lambda_S v_S^2 \end{pmatrix} \begin{pmatrix} \phi \\ \phi_S \end{pmatrix} \\ &\equiv \frac{1}{2} \begin{pmatrix} \phi & \phi_S \end{pmatrix} \begin{pmatrix} M_{11} & M_{12} \\ M_{12} & M_{22} \end{pmatrix} \begin{pmatrix} \phi \\ \phi_S \end{pmatrix} \end{aligned}$$

The mass spectrum of m_{h_1} and m_{h_2} is

$$\begin{aligned} m_{h_1}^2 &= M_{11} \cos^2\alpha + M_{22} \sin^2\alpha - 2M_{12} \cos\alpha \sin\alpha, \\ m_{h_2}^2 &= M_{11} \sin^2\alpha + M_{22} \cos^2\alpha + 2M_{12} \cos\alpha \sin\alpha, \end{aligned}$$

with the constraint

$$M_{12}(\cos^2\alpha - \sin^2\alpha) + \cos\alpha \sin\alpha (M_{11} - M_{22}) = 0.$$

2. Branching ratio of CLFV

The branching ratio for $\ell_i \to \ell_j \gamma$ is calculated as

$$\mathrm{Br}(\ell_i \to \ell_j \gamma) = \frac{48\pi^3 \alpha_{\mathrm{em}} |A_D|^2}{G_F^2} \mathrm{Br}(\ell_i \to \ell_j \overline{\nu}_j \nu_i)$$

$$A_D = -\sum_\alpha g_{i\alpha}^* g_{j\alpha} C_{23}(\xi_\alpha)$$

$$\begin{aligned} C_{23} &= -\frac{i}{32\pi^2} \int_0^1 \mathrm{d}x \frac{(1-x)^2 x}{x M_\alpha^2 + (1-x) m_{H^\pm}^2} \\ &= -\frac{i}{32\pi^2 m_{H^\pm}^2} \frac{1 - 6\xi + 3\xi^2 + 2\xi^3 - \xi^2 \ln \xi}{6(\xi - 1)^4} \equiv -\frac{i}{32\pi^2 m_{H^\pm}^2} F(\xi), \end{aligned}$$

where $m_{H^\pm}$ is the mass of the charged scalar field $H^\pm$ and the quantity ξ is defined as $\xi \equiv m_{N_\alpha}^2 / m_{H^\pm}^2$.

3. CLFV suppression

$$\mathbf{A}_D = \frac{i}{32\pi^2 m_{H^\pm}^2} g\mathbf{F}g^\dagger = \frac{i}{32\pi^2 m_{H^\pm}^2} U_{\rm PMNS}\mathcal{M}_\nu \Lambda^{-1}\mathbf{F}U_{\rm PMNS}^\dagger,$$

where $\mathbf{F}$ is defined as $\mathbf{F} = \mathrm{diag}(F(\xi_1), F(\xi_2), F(\xi_3))$.

Since $\mathcal{M}_\nu$, Λ^{-1}, $\mathbf{F}$ are all diagonalized matrices, we can denote

$$D \equiv \mathcal{M}_\nu \Lambda^{-1}\mathbf{F} = \mathrm{diag}(d_1, d_2, d_3),$$

where

$$d_i = \frac{\mathcal{M}_{\nu i} F(\xi_i)}{\Lambda_i}.$$

The $\mu \to e\gamma$ contribution in $\mathbf{A}_D$ is

$$(\mathbf{A}_D)_{12} = \frac{i}{32\pi^2 m_{H^\pm}^2}\left[c_{12}c_{13}c_{23}s_{12}(d_2 - d_1) + e^{-i\delta_{CP}} s_{13}s_{23}c_{13}(d_3 - c_{12}^2 d_1 - s_{12}^2 d_2)\right].$$